Table I. Chemical Shifts of Even Diphenylpolyenes

DPN	C-1	C-2	C-3	C-4	ipso	ortho	meta	para
2	128.4				137.0	126.4	128.7	127.6
4	132.6	129.4			137.0	126.3	128.7	127.6
6	132.4	129.3	133.8		137.0	126.3	128.7	127.6
8	132.4	129.4	133.7	133.6	137.1	126.3	128.7	127.6

concentrations without crown ether. The spectral data were as follows:

(1,3-Diphenylpropenyl)potassium (DP3⁻K⁺). ^{1}H NMR: (*E,E* conformer) δ 4.64 (d, 2 H, J = 13.2 Hz), 5.97 (t, 2 H, J = 6.9 Hz), 6.54 (m, 4 H), 6.68 (m, 4 H), 7.12 (br s, 1 H); (*E,Z* conformer) δ 5.16 and 4.28 (d, 2 H, J = 14.3 and 10.3 Hz), 6.05 and 6.17 (t, 2 H, J = 6.9 Hz), 6.60 and 6.84 (m, 9 H).

(1,5-Diphenylpentadienyl)potassium (DP5⁻K⁺). ^{1}H NMR δ 4.85 (d, 2 H, J = 14.4 Hz), 4.95 (m, 1 H), 6.21 (t, 2 H, J = 6.7 Hz), 6.60–6.75 (m, 10 H) [lit.[34] ^{1}H NMR (ether, Li⁺): δ 4.81 (t, 1 H, J = 11.2 Hz), 5.20 (d, 2 H, J = 14.4 Hz), 6.22–7.62 (m, 12 H)].

(1,7-Diphenylheptatrienyl)potassium (DP7⁻K⁺). ^{1}H NMR: δ 5.03 (t, 2 H, J = 11.9 Hz), 5.13 (d, 2 H, J = 14.4 Hz), 6.26 (t, 1 H, J = 12.7 Hz), 6.42 (t, 2 H, J = 7.1 Hz), 6.62 (dd, 2 H, J = 13.9, 11.8 Hz), 6.80 (m, 4 H), 6.88 (m, 4 H).

(1,9-Diphenylnonatetraenyl)potassium (DP9⁻K⁺). To a 10-mm NMR tube were added 24.9 mg (0.091 mmol) of DP9-H and ca. 3.0 mL of Me_2SO-d_6. All of the compound would not go into solution until subjected to brief (5-min) sonication. The dimsylpotassium (ca. 0.4 mL of a 1.5 M solution in Me_2SO-d_6) was then added, and the spectra were recorded. ^{1}H NMR: 5.08 (t, 1 H, J = 12.2 Hz), 5.20 (t, 2 H, J = 12.2 Hz), 5.38 (d, 2 H, J = 14.4 Hz), 6.22 (t, 2 H, J = 12.5 Hz), 6.59 (t, 2 H, J = 6.7 Hz), 6.67 (dd, 2 H, J = 14.4, 11.7 Hz), 6.93–6.99 (m, 8 H). The spectrum was unchanged upon addition of ca. 0.5 mL of 2.6 M 18-crown-6 in Me_2SO-d_6.

(1,11-Diphenylundecapentaenyl)potassium (DP11⁻K⁺). Dimsylpotassium (0.5 mL of a 2.5 M solution in Me_2SO-d_6) was added to 3 mL of Me_2SO-d_6 containing 28.2 mg (0.094 mmol) of DP11-H in a 10-mm NMR tube. The mixture was transferred via gas-tight syringe and filtered directly into a second 10-mm NMR tube through a 5-μm filter. ^{1}H NMR: δ 5.17 (t, 2 H, J = 12.0 Hz), 5.37 (t, 2 H, J = 12.0 Hz), 5.58 (d, 2 H, J = 14.8 Hz), 6.16 (m, 1 H), 6.23 (t, 2 H, J = 12.4 Hz), 6.74 (m, 4 H), 7.04–7.45 (m, 8 H).

(1,13-Diphenyltridecahexaenyl)potassium (DP13⁻K⁺). The anion was generated from 17.4 mg (0.054 mmol) of DP13-H in 3 mL of Me_2SO-d_6 and 0.5 mL of 2.5 M dimsylpotassium in a 10-mm NMR tube. As in the previous example, filtration was required to provide an acceptable sample. ^{1}H NMR: δ 5.22 (m, 1 H), 5.29 (t, 2 H, J = 11.7 Hz), 5.52 (t, 2 H, J = 12.3 Hz), 5.75 (d, 2 H, J = 15.0 Hz), 6.16 (m, 2 H), 6.25 (t, 2 H, J = 12.6 Hz), 6.75 (dd, 2 H, J = 14.4, 11.7 Hz), 6.81 (m, 2 H), 7.02–7.48 (m, 8 H).

Procedure for DP2, DP4, DP6, and DP8. A typical procedure is as follows: A 0.10–0.30-mmol sample of the hydrocarbon was dissolved in 1.0–1.5 mL of Me_2SO-d_6 in a 5-mm NMR tube. ^{13}C chemical shifts were determined from the HETCOR spectrum utilizing DP6 as a representative sample. The results are reported in Table I.

Acknowledgment. Support of this research by the U.S. Department of Energy through Grant No. DE-FG05-85ER45194 is gratefully acknowledged. Thanks are also due to Prof. William Eberhardt for lively and enlightening discussions.

^{1}H NMR Resonance Assignment of the Active Site Residues of Paramagnetic Proteins by 2D Bond Correlation Spectroscopy: Metcyanomyoglobin

Liping P. Yu, Gerd N. La Mar,* and Krishnakumar Rajarathnam

Contribution from the Department of Chemistry, University of California, Davis, California 95616. *Received May 8, 1990*

Abstract: Two-dimensional conventional magnitude COSY, phase-sensitive pure absorption DQF-COSY, and HOHAHA experiments have been successfully applied to paramagnetic low-spin ferric sperm whale metcyanomyoglobin to identify the spin systems of the side chains of the residues located in the heme cavity. The assignments from the present bond correlation spectroscopy for the residues of Ile FG5/99, Phe CD1/43, His F8/93, Val E11/68, and heme itself confirm the assignments made previously by interpreting nuclear Overhauser effect, NOE, data on the basis of the X-ray crystal structure. The spin system of a Leu side chain with strongly hyperfine shifted resonances has been unambiguously identified with a combination of COSY and HOHAHA spectra and assigned to the Leu F4/89 residue located in the heme pocket on the proximal side, for which the initial partial assignments are shown to be invalid. The incorrect earlier assignments resulted from a difference between the solution and crystal orientation of the side chain. Molecular modeling and dipolar shift calculations upon rotating the Leu F4/89 side chain about the C_β–C_γ bond by $\sim$120° lead to an orientation consistent with both the observed dipolar shifts and NOEs to the heme. The methods of bond correlation spectroscopy are qualitatively evaluated and shown to be able to identify cross peaks from pairs of protons experiencing very rapid paramagnetic relaxation rates with T_1s as short as $\sim$20 ms and line widths as large as $\sim$100 Hz. Preliminary 2D bond correlation spectroscopic data on the cyano complex of horseradish peroxidase suggest that J cross peaks can identify residues in even larger paramagnetic heme proteins. The various methods considered, however, differ significantly in their information content, with the magnitude COSY map providing the optimal information on the strongly relaxed protons. In particular, the double quantum filter is found to strongly discriminate against rapidly relaxed, broad, and spin-coupled resonances, making DQF-COSY experiments virtually useless for the protons closest to the iron. The variable-temperature HOHAHA and COSY maps serve to define complete spin systems. Therefore, it is clear that 2D bond correlation spectroscopy can be profitably applied to paramagnetic macromolecules and that, along with the 2D nuclear Overhauser effect spectroscopy (NOESY) [Emerson, S. D.; La Mar, G. N. *Biochemistry* **1990**, *29*, 1545–1556], the solution structures of paramagnetic molecules, at least low-spin ferric molecules, should be determinable with 2D NMR techniques in a fashion now attainable for diamagnetic molecules.

Introduction

It has long been recognized that the information content of the ^{1}H NMR spectra of paramagnetic proteins is very high, but the needed resonance assignments and interpretative basis of the hyperfine shifts are much more complicated than for diamagnetic proteins.[1-7] Originally, it was thought that 2D NMR methods used for diamagnetic molecules[8] will have little applicability to

(1) La Mar, G. N. In *Biological Applications of Magnetic Resonances*; Shulman, R. G., Ed.; Academic Press: New York, 1979; pp 61–159.

0002-7863/90/1512-9527$02.50/0

paramagnetic molecules, particularly, for the fast relaxing protons near the paramagnetic center. Therefore, NMR resonance assignments for the hyperfine shifted resonances in paramagnetic proteins have relied primarily on comparisons with model compounds,[1-3] analysis of differential paramagnetic relaxation,[3,9] isotope labeling,[2,10,11] and saturation transfer from a protein form with assigned resonances.[12,13]

Over the past decade, it has been demonstrated that the 1D nuclear Overhauser effect[14] (NOE) can be effectively used for resonance assignments of even strongly paramagnetic metalloproteins, provided that information is available on the likely structure of the complex.[9,15-17] More recently, we have demonstrated that 95% of the protons within 7.5 Å of the spin $S = 1/2$ ferric iron of metcyanomyoglobin (metMbCN)[18] can be assigned on the basis of a 2D NOESY map[19] by using the X-ray crystal coordinates[20] to interpret the cross peaks. These assignments were then used to determine for the first time the orientation of the magnetic axes in solution, and this orientation was proposed to provide a very sensitive probe of steric tilt of bound ligand.[6] Thus, the full utility of NOESY maps, at least in low-spin ferric systems, has been clearly established.

There has been much less work on paramagnetic molecules using bond correlation 2D methods of COSY,[18,21,22] DQF-COSY,[18,23,24] and TOCSY/HOHAHA.[18,25,26] The feasibility of COSY in inorganic lanthanide complexes has been documented,[27] but applications to paramagnetic proteins have addressed only the main-chain protons and side chains remote from the iron.[28,29] For metMbCN, preliminary COSY studies revealed cross peaks only for residues with large coupling (e.g., vinyl groups) and >6 Å from the iron,[19,30] although the severe limitation of the available instrumentation for our earlier study[19] did not constitute a crucial test of the method.

Resonance assignments derived from the interpretation of NOEs on the basis of X-ray coordinate data[19] have two severe limitations: (1) crystal structures must be available and (2) it assumes that the solution structure is identical with the crystal structure. However, solution structures and crystal structures have been reported to be different for a number of molecules,[7,31] and X-ray crystal structures are not readily available for most hemoprotein genetic variants and synthetic point mutants. Hence, in order to put the solution structure determination of paramagnetic molecules on a basis comparable to that of diamagnetic molecules,[8] the assignments of amino acid side chains should be independent of tertiary structure. Of considerable interest is the question whether the complete 3D solution structure determination of paramagnetic proteins can be effected essentially the same way as for diamagnetic molecules, whose spin systems of individual residues are uniquely identified first with bond correlation spectroscopy, that is, either COSY, MQF-COSY, or HOHAHA, followed by sorting out their spatial locations with NOESY.[8,32-34]

HOHAHA, COSY, and DQF-COSY experiments[21-26] are well documented in the studies of diamagnetic systems with slow intrinsic spin–lattice relaxation, narrow resonance line widths, and small spectral windows. In paramagnetic systems, however, paramagnetically induced relaxation both broadens resonance lines and significantly increases the intrinsic spin–lattice relaxation rates. The rapidly relaxed signals also significantly die away even during a short spin-locking period in TOCSY/HOHAHA experiments. The antiphase components in the COSY and DQF-COSY experiments may partially or wholly cancel for broadened lines, particularly if digital resolution is inadequate. Furthermore, paramagnetic molecules exhibit larger chemical shift dispersion, which is advantageous for spectral resolution, but demand strong spin-locking fields and large data sets for adequate digital resolution. These problems, however, influence the various protons in a paramagnetic molecule in a highly differential manner.

The low-spin ferric hemoproteins represent an important subclass of paramagnetic metalloproteins whose ^{1}H NMR spectral parameters contain a wealth of structural information.[1-7] They comprise the heavily studied ferricytochromes,[4,5,28,29] metcyanomyoglobins, and hemoglobins,[6,9,11,19,35] and the cyanide complex of resting state heme peroxidases.[16,17] As a prototype molecule for this class of proteins, we target in this report the unambiguous assignment of the side chain for residues closest to the iron in sperm whale metcyanomyoglobin (metMbCN), for which assignments had been proposed[19] based upon interpreting a NOESY map in terms of crystal coordinates for MbCO. The important residues are the heme itself, His F8/93, Phe CD1/43, Ile FG5/99, Val E11/68, and Leu F4/89, which are key residues for establishing the orientation of the magnetic axes.[6,36] We address here

(2) Satterlee, J. D. *Annu. Rep. NMR Spectrosc.* **1985**, *17*, 79–178.
(3) Bertini, I.; Luchinat, C. *NMR of Paramagnetic Molecules in Biological Systems*; The Benjamin/Cummings: Menlo Park, CA, 1986.
(4) Senn, H.; Wüthrich, K. *Q. Rev. Biophys.* **1985**, *18*, 111–134.
(5) Williams, G.; Moore, G. R.; Porteous, R.; Robinson, M. N.; Soffe, N.; Williams, R. J. P. *J. Mol. Biol.* **1985**, *183*, 409–428.
(6) Emerson, S. D.; La Mar, G. N. *Biochemistry* **1990**, *29*, 1556–1566.
(7) Feng, Y.; Roder, H.; Englander, S. W. *Biochemistry* **1990**, *29*, 3494–3504.
(8) Wüthrich, K. *NMR of Proteins and Nucleic Acids*; Wiley: New York, 1986.
(9) Emerson, S. D.; Lecomte, J. T. J.; La Mar, G. N. *J. Am. Chem. Soc.* **1988**, *110*, 4176–4182.
(10) de Ropp, J. S.; La Mar, G. N.; Smith, K. M.; Langry, K. C. *J. Am. Chem. Soc.* **1984**, *106*, 4438–4444.
(11) Mayer, A.; Ogawa, S.; Shulman, R. G.; Yamane, T.; Cavaleiro, J. A. S.; Rocha Gonsalves, A. M. d'A.; Kenner, G. W.; Smith, K. M. *J. Mol. Biol.* **1974**, *86*, 749–756.
(12) Keller, R. M.; Wüthrich, K. *Biochem. Biophys. Res. Commun.* **1978**, *83*, 1132–1139.
(13) Boyd, J.; Moore, G. R.; Williams, G. *J. Magn. Reson.* **1984**, *58*, 511–516.
(14) Neuhaus, D.; Williamson, M. *The Nuclear Overhauser Effect in Structural and Conformational Analysis*; VCH Publishers: New York, 1989.
(15) Unger, S. W.; Lecomte, J. T. J.; La Mar, G. N. *J. Magn. Reson.* **1985**, *64*, 521–526.
(16) Thanabal, V.; de Ropp, J. S.; La Mar, G. N. *J. Am. Chem. Soc.* **1987**, *109*, 265–272.
(17) Thanabal, V.; de Ropp, J. S.; La Mar, G. N. *J. Am. Chem. Soc.* **1987**, *109*, 7516–7525.
(18) Abbreviations: Mb, myoglobin; Hb, hemoglobin; metMb, metmyoglobin (ferric); HRP, resting state horseradish peroxidase (ferric); COSY, two-dimensional correlated spectroscopy; MCOSY, conventional magnitude two-dimensional correlated spectroscopy; PCOSY, two-dimensional purged correlated spectroscopy; DQF-COSY, two-dimensional double quantum filtered correlated spectroscopy; MQF-COSY, two-dimensional multiple quantum filtered correlated spectroscopy; TOCSY, two-dimensional total correlation spectroscopy; HOHAHA, two-dimensional homonuclear Hartmann–Hahn spectroscopy; NOE, nuclear Overhauser effect; NOESY, two-dimensional nuclear Overhauser effect spectroscopy; DSS, 2,2-dimethyl-2-silapentane-5-sulfonate; ppm, parts per million; FID, free induction decay.
(19) Emerson, S. D.; La Mar, G. N. *Biochemistry* **1990**, *29*, 1545–1556.
(20) Kuriyan, J.; Wilz, S.; Karplus, M.; Petsko, G. A. *J. Mol. Biol.* **1986**, *192*, 133–154.
(21) Marion, D.; Wüthrich, K. *Biochem. Biophys. Res. Commun.* **1983**, *113*, 967–974.
(22) Bax, A.; Freeman, R.; Morris, G. *J. Magn. Reson.* **1981**, *42*, 164–168.
(23) Edwards, M. W.; Bax, A. *J. Am. Chem. Soc.* **1986**, *108*, 918–923.
(24) Muller, N.; Ernst, R. R.; Wüthrich, K. *J. Am. Chem. Soc.* **1986**, *108*, 6482–6492.
(25) Braunschweiler, L.; Ernst, R. R. *J. Magn. Reson.* **1983**, *53*, 521–528.
(26) Bax, A.; Davis, D. G. *J. Magn. Reson.* **1985**, *65*, 355–360.
(27) Jenkins, B. G.; Lauffer, R. B. *J. Magn. Reson.* **1988**, *80*, 328–336.
(28) Feng, Y.; Englander, S. W. *Biochemistry* **1990**, *29*, 3505–3509.
(29) Feng, Y.; Roder, H.; Englander, S. W.; Wand, A. J.; Di Stefano, D. L. *Biochemistry* **1989**, *28*, 195–203.
(30) Yamamoto, Y.; Osawa, A.; Inoue, Y.; Chujo, R.; Suzuki, T. *FEBS Lett.* **1989**, *247*, 263–267.
(31) Williams, G.; Clayden, N. J.; Moore, G. R.; Williams, R. J. P. *J. Mol. Biol.* **1985**, *183*, 447–460. Chazin, W. J.; Hugli, T. E.; Wright, P. E. *Biochemistry* **1988**, *27*, 9139–9148. Lin, S.-L.; Stern, E. A.; Kalb (Gilboa), A. J.; Zhang, Y. *Biochemistry* **1990**, *29*, 3599–3603.
(32) Dyson, H. J.; Holmgren, A.; Wright, P. E. *Biochemistry* **1989**, 28, 7074–7087.
(33) Dalvit, C.; Wright, P. E. *J. Mol. Biol.* **1987**, *194*, 313–327.
(34) Wand, A. J.; Di Stefano, D. L.; Feng, Y.; Roder, H.; Englander, S. W. *Biochemistry* **1989**, *28*, 186–194.
(35) Morrow, J. S.; Gurd, F. R. N. *CRC Crit. Rev. Biochem.* **1975**, *3*, 221–287.

the following questions: (1) Can assignments for these amino acid side chains in the heme cavity be made solely by spin correlation through J coupling? (2) Which of the most commonly used spin correlation experiments for a diamagnetic molecule is the most effective one for a paramagnetic molecule? (3) Are the assignments from the bond correlation spectroscopy consistent with those determined solely from the predicted NOE data?[19] (4) What are the structural consequences of the new altered assignments? (5) What are the prospects of resonance assignments through bond correlation spectroscopy for larger paramagnetic molecules?

Experimental Procedures

Sample Preparation. Sperm whale Mb and horseradish peroxidase, HRP (type VI), were purchased from Sigma Chemical Co. as lyophilized salt-free powders and used without further purification. ^2H_2O solutions of 4 mM metcyanomyoglobin, metMbCN, pH 8.6, were prepared as described previously.[19] The HRPCN sample was prepared by addition of excess KCN to a 3 mM ^2H_2O solution of horseradish peroxidase, pH 7.0. The sample pH was adjusted with 0.2 M solutions of NaO^2H or ^2HCl and measured in a NMR tube by an Ingold microcombination electrode. The reported pH values were uncorrected for the isotope effect. Labile protons were completely exchanged by long-time storage in ^2H_2O at 4 °C.

^1H NMR Measurements. All the 2D experiments were carried out on a General Electric Ω 500-MHz spectrometer. The phase-sensitive COSY,[21] PCOSY,[18,37] DQF-COSY,[23,24] and HOHAHA[25,26] spectra employed the method described by States et al.[38] to provide quadrature detection in the t1 dimension. The MLEV-17 mixing scheme[26] was used in the HOHAHA experiments, and the MLEV-17 pulse sequence was written in such a way so that the magnetization was aligned along the effective axis of rotation of the 180° composite pulse for obtaining optimal sensitivity.[39] The conventional n-type COSY spectra were collected with magnitude display[22,40] and designated as MCOSY hereafter. Solvent suppression, when required, was achieved by direct saturation in the relaxation delay period.

For the metMbCN sample, 512 blocks were collected with spectral width of 15 504 Hz, and ~128 scans were accumulated for each block with free induction decays (FID) of 1024 complex data points. The 90° pulse width was 27 ms for the HOHAHA and 13 ms for the other 2D experiments. Eight dummy scans were used, and a recycle delay of 1.6 s including acquisition was employed. The 2D data were processed on a μ-Vax II computer with a Fortran program FTNMR written by Dr. Dennis Hare. The time domain data were normally multiplied in the t1 and t2 dimensions by sinebell window function with phase shifts of 30° for the HOHAHA, 15° for DQF-COSY, and 0° for the other 2D spectra and were zero-filled to obtain 2K × 2K real data points with digital resolution of ~7.6 Hz per point. 2D data processing different from the above will be indicated in appropriate figure captions. For the HRPCN sample, 256 blocks were collected with spectral width of 26 315 Hz, and ~400 scans were accumulated for each block with an FID of 1024 complex data points. The collected data were processed to obtain 2K × 2K real data points with digital resolution of ~13 Hz per point. The 90° pulse width of this sample was 7 ms for the MCOSY and 18 ms for the HOHAHA. Chemical shifts for all the spectra were referenced to 2,2-dimethyl-2-silapentane-5-sulfonate (DSS) through the residual water resonance.

Calculation of Dipolar Shifts of Leu F4. The methyls of the Leu F4 were rotated about the C_β–C_γ bond as it has the least energy barrier.[20] The rest of the Leu F4 residue is assumed to be unchanged. Rotation of the Leu F4 side chain about the C_β–C_γ bond and the calculations of the interproton distances were performed by using the MIDAS program (University of California, San Francisco) on a IRIS 4D/50GT work station (Silicon Graphics). Calculations of the dipolar chemical shifts were performed on a μ-Vax II workstation. The unit cell coordinates of the crystal structure of MbCO[20] were converted into iron-centered heme symmetry coordinates by the SMAX program.[6] The program GLOBMIN was used to obtain the Euler angles which determine the magnetic axes, the input data being the symmetry coordinates of protons and their observed dipolar chemical shifts.[6] The program CALPS calculates the dipolar chemical shifts of protons for the given Euler angles.[6] The computer programs SMAX, CALPS, and GLOBMIN were written by S. D. Emerson, and these were described in detail previously.[6]

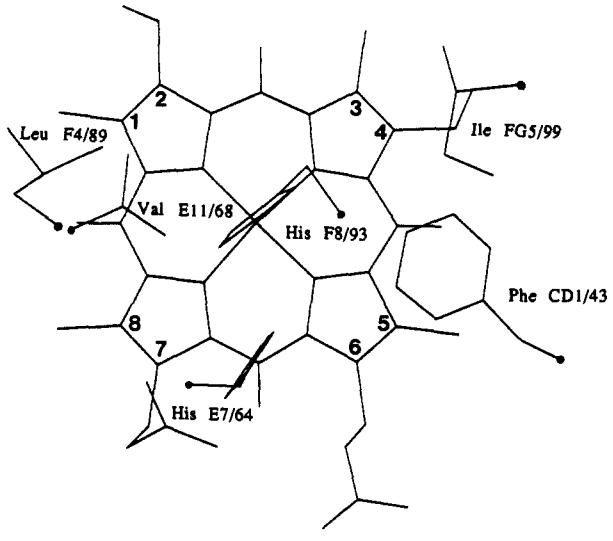

Figure 1. Schematic representation of the spatial disposition of the targeted amino acid side chains in the heme cavity of metMbCN. The pointed peak of each surface indicates the location of the C_α for each residue.

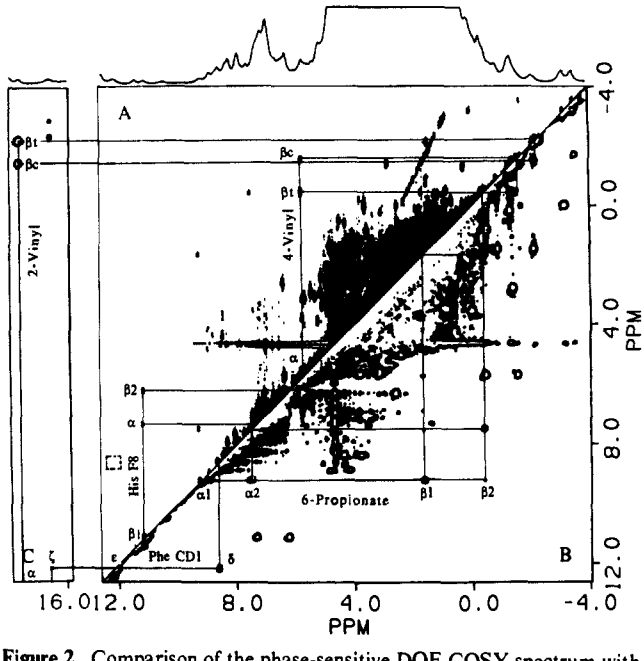

Figure 2. Comparison of the phase-sensitive DQF-COSY spectrum with the MCOSY spectrum of metMbCN at 35 °C: (A) is the phase-sensitive DQF-COSY spectrum and (B) and (C) are the MCOSY spectrum. (C) is plotted at a lower contour level than (B). Spin system connectivities are drawn for residues of His F8/93, Phe CD1/43, heme 6-propionate group, and heme 2- and 4-vinyl groups. The small dotted-line squares indicate the cross peaks which are observed only at a lower contour level. The 1D spectrum of this sample is also drawn along the F_2 axis.

The predicted chemical shift, δ_{pre}, for a noncoordinated residue proton, relative to DSS, is given by

$$\delta_{pre} = \delta_{dia} + \delta_{dip}(\text{calc}) \quad (1)$$

where δ_{dia} is the reported diamagnetic chemical shift for MbCO[33] and δ_{dip}(calc) is the calculated dipolar chemical shift by using the published magnetic anisotropy values, the magnetic axes determined previously, and the coordinates of the residue.[6] For the case of the X-ray side-chain orientation of Leu F4, δ_{dip}(calc) has been determined,[6] and the total shift is designated by δ^*_{pre}. We calculate now δ_{dip}(calc) for the Leu F4 side chain at 30° intervals for the rotation about the C_β–C_γ bond and compare the predicted total shifts with the observed shifts; the best fit is indicated by δ^+_{pre}. It was found that ring current effects were negligible with C_β–C_γ bond rotations; hence δ_{dia} remained constant.

(36) His E7/64 is excluded because it does not affect the determination of the susceptibility tensor; see ref 6.

(37) Marion, D.; Bax, A. *J. Magn. Reson.* **1988**, *80*, 528–533.
(38) States, D. J.; Haberkorn, R. A.; Reuben, D. J. *J. Magn. Reson.* **1982**, *48*, 286–292.
(39) Rance, M. *J. Magn. Reson.* **1987**, *74*, 557–564.
(40) Bax, A. *Two-Dimensional Nuclear Magnetic Resonance in Liquids*; Delft University Press: D. Reidel Publishing Company: London, England, 1984.

Table I. Chemical Shifts, Relaxation Times, and Line Widths for the Spin Systems of the Residues in the Heme Pocket in Sperm Whale Metcyanomyoglobin

residues	spins	chemical shifts[a] (ppm)	T_1[b] (ms)	line width[c] (Hz)
His F8/93	$C_\alpha H$	7.3	130	
	$C_{\beta 1} H$	11.1	75	49
	$C_{\beta 2} H$	6.2	(120)	
Phe CD1/43	$C_\zeta H$	16.6	20	81
	$C_\epsilon Hs$	12.1	47	62
	$C_\delta Hs$	8.6		
Val E11/68	$C_\alpha H$	−2.1	110	
	$C_\beta H$	1.5	(200)	
	$C_{\gamma 1} H_3$	−0.9	56	
	$C_{\gamma 2} H_3$	−0.7	35	
Ile FG5/99	$C_\alpha H$	2.5		
	$C_\beta H$	0.0	(280)	
	$C_{\gamma 1} H$	−8.7	65	94
	$C_{\gamma 2} H$	−1.6	119	
	$C_\gamma H_3$	−3.2	199	32
	$C_\delta H_3$	−3.5	188	34
Leu F4/89	$C_\alpha H$	8.3		
	$C_{\beta 1} H$	4.4		
	$C_{\beta 2} H$	3.7		
	$C_\gamma H$	5.7		
	$C_{\delta 1} H_3$	3.8		
	$C_{\delta 2} H_3$	3.1		
heme 2-vinyl	$C_\alpha H$	17.6	108	40
	$C_{\beta c} H$	−1.5	189	
	$C_{\beta t} H$	−2.3	169	
heme 4-vinyl	$C_\alpha H$	5.7		
	$C_{\beta c} H$	−1.5		
	$C_{\beta t} H$	−0.4		
heme 6-propionate	$C_{\alpha 1} H$	9.2		50
	$C_{\alpha 2} H$	7.5		
	$C_{\beta 1} H$	1.7		
	$C_{\beta 2} H$	−0.4		

[a] Assignments were taken from ref 19 except for Leu F4/89 residue. The chemical shifts are at 35 °C. [b] Taken from refs 9 and 19 and measured at 40 °C. The values in parentheses are the estimated ones on the basis of $T_1 \propto R_{Fe}^6$, where R is the distance from the proton of interest to the heme iron, and the estimated T_1 = 4 ms for $R_{Fe} \sim 3.4$ Å and T_1 = 300 ms for $R_{Fe} \sim 7.0$ Å. [c] Only the line widths for the resolved peaks are measured.

Table II. Comparison of the Results for Sperm Whale Metcyanomyoglobin Collected with the Conventional Magnitude COSY (MCOSY), Phase-Sensitive DQF-COSY, and HOHAHA[a]

residues	spin correlation	DQF-COSY	MCOSY	HOHAHA
His F8/93	$C_{\beta 1} H$–$C_{\beta 2} H$	+	+	+
	$C_{\beta 1} H$–$C_\alpha H$	+	+	+
	$C_{\beta 2} H$–$C_\alpha H$	−	*c*	+
Phe CD1/43	$C_\zeta H$–$C_\epsilon Hs$	−	+	−
	$C_\epsilon H$–$C_\delta Hs$	*d*	+	+
Val E11/68	$C_\alpha H$–$C_\beta H$	+[b]	+	+
	$C_\beta H$–$C_{\gamma 1} H_3$	+	+	+
	$C_\beta H$–$C_{\gamma 2} H_3$	+	+	*d*
Ile FG5/99	$C_{\gamma 1} H$–$C_{\gamma 2} H$	−	+	−
	$C_{\gamma 1} H$–$C_\delta H_3$	−	+	+
	$C_{\gamma 2} H$–$C_\delta H_3$	+	+	+
	$C_{\gamma 1} H$–$C_\beta H$	−	−	−
	$C_{\gamma 2} H$–$C_\beta H$	−	+	*d*
	$C_\beta H$–$C_\gamma H_3$	+	+	+
	$C_\alpha H$–$C_\beta H$	+[b]	+	+
Leu F4/89	$C_\alpha H$–$C_{\beta 1} H$	+[e]	+	+
	$C_\alpha H$–$C_{\beta 2} H$	+	+	+
	$C_{\beta 1} H$–$C_{\beta 2} H$	+	*c*	+
	$C_{\beta 1} H$–$C_\gamma H$	+	+	+
	$C_{\beta 2} H$–$C_\gamma H$	+	+	+
	$C_\gamma H$–$C_{\delta 1} H_3$	+	+	+
	$C_\gamma H$–$C_{\delta 2} H_3$	+	+	+
heme 2-vinyl	$C_\alpha H$–$C_{\beta c} H$	+[b]	+	*f*
	$C_\alpha H$–$C_{\beta t} H$	+[b]	+	+
	$C_{\beta c} H$–$C_{\beta t} H$	−	+	*g*
heme 4-vinyl	$C_\alpha H$–$C_{\beta c} H$	+[b]	+	+
	$C_\alpha H$–$C_{\beta t} H$	+[b]	+	+
	$C_{\beta c} H$–$C_{\beta t} H$	−	+	+
heme 6-propionate	$C_{\alpha 1} H$–$C_{\alpha 2} H$	+	+	+
	$C_{\alpha 1} H$–$C_{\beta 1} H$	+	+	+
	$C_{\alpha 1} H$–$C_{\beta 2} H$	−	+	+
	$C_{\alpha 2} H$–$C_{\beta 1} H$	−	−	+
	$C_{\alpha 2} H$–$C_{\beta 2} H$	+	+	+
	$C_{\beta 1} H$–$C_{\beta 2} H$	+	+	+

[a] The positive sign, +, means that the spin correlations are observed, and the negative sign, −, means that the spin correlations are not observed in the experiment. [b] The cross peaks were reported before (ref 19). [c] Too close to the diagonal to be determined. [d] Seen at a lower contour level. [e] The cross peak was observed but incorrectly assigned to $C_\gamma H$–$C_{\delta 2} H_3$ (ref 19). [f] Do not show up because of weak spin-locking field strength. [g] Not seen for the mixing of weak spin-locking field strength. [g] Not seen for the mixing times of 25 and 35 ms, and because it is located too close to the diagonal where there is a negative dip.

Results

The Heme. The heme structure and the residues in close contact with heme are illustrated in Figure 1. The current DQF-COSY map (Figure 2A) reveals all the 6-propionate resonance cross peaks except $C_{\alpha 1} H$:$C_{\beta 2} H$ and $C_{\alpha 2} H$:$C_{\beta 1} H$; the former cross peak is additionally detected in the MCOSY (Figure 2B), although only weakly. The complete 6-propionate spin system is traced in Figure 2B and confirms the previously NOE based assignments. The 7-propionate resonances occur in the crowded aliphatic region and were not further pursued by bond correlation spectroscopy since detection is not in question.

While the spin connectivities between the pairs of $C_\alpha H$:$C_{\beta t} H$ and $C_\alpha H$:$C_{\beta c} H$ cross peaks for both vinyls are readily observed in either DQF-COSY or MCOSY spectra (Figure 2), the latter map provides additional cross peaks between $C_{\beta t} H$ and $C_{\beta c} H$ as traced in Figure 2. In the HOHAHA spectra, full spin connectivities of the 4-vinyl are detected. For the 2-vinyl, however, only one weak cross peak from the pair with a larger J coupling constant (i.e., $C_\alpha H$:$C_{\beta 1} H$) is detected in the HOHAHA spectra (not shown). This is due to chemical shift dispersion (~10 kHz at 500 MHz), which requires a much stronger B_1 spin-lock field than available to us on the GE Ω 500-MHz spectrometer (~27 μs 90° pulse width at maximal power for this sample). The chemical shifts of the ^1H resonances, along with their available longitudinal relaxation times and line widths at half-height for the resolved resonances, are listed in Table I. Table II summarizes the comparative results for detecting bond connectivities with DQF-COSY, MCOSY, and HOHAHA experiments.

Phe CD1/43. This CD1 residue is located very close to the paramagnetic center and experiences severe paramagnetic relaxation: the $C_\zeta H$ exhibits T_1 ~20 ms and line width ~80 Hz. Additionally, the $C_\epsilon Hs$ and $C_\delta Hs$ experience line broadening from ring flipping that averages their chemical shifts.[9] The side-chain COSY cross peaks had not been detected previously.[19] Therefore, the observability of the cross peaks for this residue with 2D bond correlation spectroscopy constitutes one of the most stringent tests of these methods in low-spin ferric hemoproteins. However, we are presently able to detect all the spin connectivities for this aromatic ring in the MCOSY, as traced in Figure 2B,C, although the intensity for the cross peak $C_\zeta H$:$C_\epsilon Hs$ is very low. In the DQF-COSY map, the $C_\zeta H$:$C_\epsilon Hs$ cross peak is not observed, while the cross peak $C_\epsilon Hs$:$C_\delta Hs$ is only weakly seen at lower contour level (Figure 2A).

Ile FG5/99. The $C_{\gamma 1} H$ resonance (at −8.7 ppm) of this residue experiences strong paramagnetic relaxation with T_1 ~65 ms and line width ~95 Hz, the third broadest in the ^1H NMR spectrum of metMbCN (the two broader are the His F8 ring $C_\epsilon H$ and $C_\delta H$). The cross peaks for the pairs $C_{\gamma 1}$:$C_{\gamma 2} H$ and $C_{\gamma 1} H$:$C_\delta H_3$ have not been previously observed.[19] These cross peaks again provide a crucial test of the applicability of 2D methods. Both of these cross peaks are clearly observed in the present MCOSY spectrum (Figure 3A), although their intensities are low relative to others. In the HOHAHA spectrum, the cross peak $C_{\gamma 1} H$:$C_\delta H_3$ is also observed; however, the cross peak $C_{\gamma 1} H$:$C_{\gamma 2} H$ is missing (Figure 3B). The $C_\alpha H$ resonance is located in the crowded aliphatic region, and therefore its assignment from the MCOSY spectrum alone is ambiguous due to resonance overlap. However, the HOHAHA spectrum shows the relayed peak from the $C_\gamma H_3$ to $C_\alpha H$, thus making the assignment of the $C_\alpha H$ unambiguous

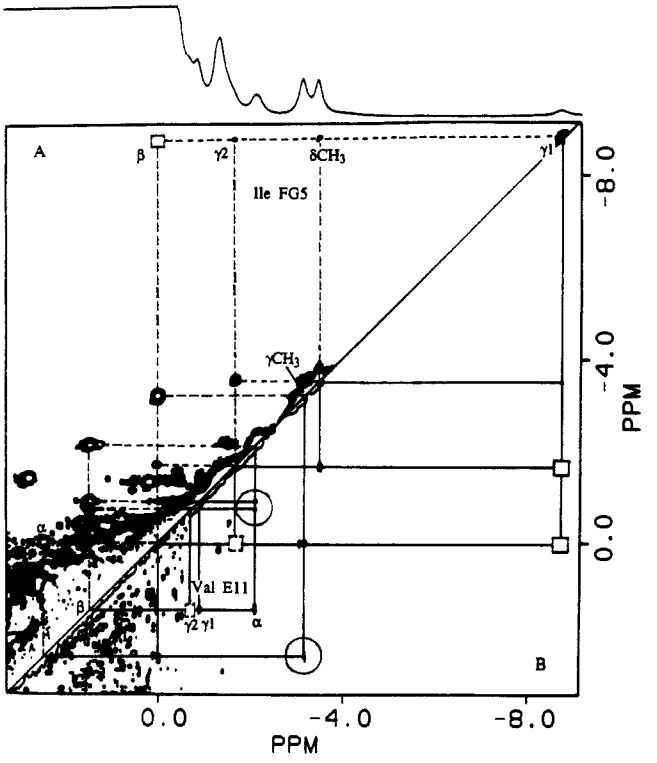

Figure 3. Comparison of the phase-sensitive HOHAHA spectrum with the MCOSY spectrum of metMbCN at 35 °C: (A) the MCOSY spectrum and (B) the phase-sensitive HOHAHA spectrum, collected with 25-ms mixing time and with a trim pulse length of 100 μs. Spin system connectivities are drawn for residues of Ile FG5/99 and Val E11/68. The small solid-line squares indicate where expected cross peaks are not observed. The small dotted-line squares indicate the cross peaks which are observed only at a lower contour level. The small circles indicate the relayed cross peaks. The spin system for Ile FG5/99 is labeled in panel A, and the spin system for Val E11/68 is labeled in panel B. The 1D spectrum of this sample is also drawn along the F_2 axis.

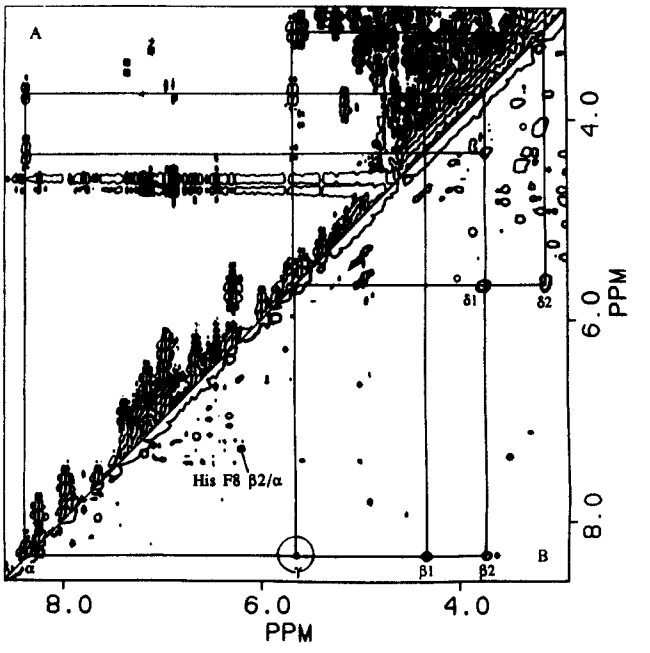

Figure 4. Comparison of portions of the phase-sensitive HOHAHA and DQF-COSY spectra of metMbCN at 35 °C: (A) the phase-sensitive DQF-COSY spectrum and (B) the phase-sensitive HOHAHA spectrum, collected with 25-ms mixing time and with a trim pulse length of 100 μs. Spin system connectivities are drawn for the residue of Leu F4/89. The small circle indicates the relayed cross peak between $C_\alpha H$ and $C_\gamma H$. In addition, one cross peak from His F8 $C_{\beta 2}H$:$C_\alpha H$ is labeled.

(Figure 3B). The MCOSY spectrum displays essentially all the spin connectivities unique for an Ile residue, except that for $C_{\gamma 1}H$:$C_\beta H$ (Figure 3). The inability to see the latter cross peak is due to the small expected J coupling constant (dihedral angle ~102°)[20] and larger line widths. Thus, present bond correlation spectroscopy data definitively confirm the previous NOE-based assignments of this residue.

His F8/93. The cross peaks $C_{\beta 1}H$:$C_\alpha H$ and $C_{\beta 1}H$:$C_{\beta 2}H$ for the His F8/93 residue are observed in both DQF-COSY and MCOSY spectra (Figure 2). The spin connectivities for this residue are drawn in Figure 2A. In the HOHAHA spectrum, in addition to these two cross peaks, that for the pair of $C_{\beta 2}H$:$C_\alpha H$ is also observed (Figure 4). Thus, the present bond correlation spectra again confirm the previously assigned[19] His F8/93 $C_\alpha H$–$C_\beta H_2$ spin system.

Val E11/68. All the experiments described here define the complete spin system connectivities as shown in Figure 3. However, the cross peak $C_\beta H$:$C_{\gamma 2}H_3$ is marginally detected in the DQF-COSY spectrum, because of the proximity of the $C_{\gamma 2}H_3$ to the iron and concomitant line broadening.[19] The intensity of this cross peak in the HOHAHA spectrum is also very low and can be seen only at a lower contour level (Figure 3B). However, MCOSY reveals a relatively strong cross peak for this pair of protons (Figure 3A). The HOHAHA spectrum moreover shows the relayed cross peaks from $C_\alpha H$ to $C_{\gamma 2}H_3$ and $C_{\gamma 1}H_3$ at a mixing time of 25 ms (Figure 3B), and the intensities of these relayed cross peaks increase slightly at a mixing time of 35 ms (not shown). Thus the HOHAHA spectra confirm the Val spin system as assigned previously based upon the NOE data.[19]

Leu F4/89. Of the side chains closest to iron, this proximal residue has allowed the fewest assignments to date.[19] An NOE between the His F8 $N_\delta H$ and an apparently unresolved methyl was interpreted[19] as arising from the $C_{\delta 2}H_3$ based upon prediction from X-ray coordinates of MbCO[20] (the Leu $C_\alpha H$ and $C_{\delta 2}H_3$ are found comparably close to the His F8 $N_\delta H$). A single COSY cross peak[19] from the proposed $C_{\delta 2}H_3$ was thought to identify the $C_\gamma H$. The difficulty in making assignments for this residue is due to the fact that its strongly hyperfine shifted ^1H resonances are still wholly within the crowded diamagnetic envelope. Collecting the HOHAHA spectra with different mixing times, along with other COSY spectra at different temperatures, we are able to uniquely identify the spin system of Leu F4/89 as shown in Figure 4. The observed relay cross peak between $C_\alpha H$ and $C_\gamma H$, as shown in Figure 4B, is key for this identification, which is missing in the DQF-COSY spectrum (Figure 4A) and the MCOSY spectrum (Figure 2B). The intensity of this relayed cross peak increases slightly with mixing time from 25 to 35 ms. The cross peak $C_\gamma H$:$C_{\beta 1}H$ is relatively weak in the DQF-COSY spectrum due to its small J coupling constant. The resonances for $C_{\delta 1}H_3$ and $C_{\beta 2}H$ overlap at this temperature, but they resolve at other temperatures (not shown). Due to the different sensitivity of the hyperfine shifts to temperature for the various ^1H resonances, even within an individual residue, the whole spin system connectivities can be easily confirmed at other temperatures, thus verifying the assignments for the Leu F4/89 side chain. It is noted that the present unambiguous assignments invalidate the previously NOE-based assignment of $C_{\delta 2}H_3$ peak.[19] We consider the origin of this problem below.

Studies of HRPCN. From the previous studies,[10,16,17] it is known that the residues in the active site in HRPCN, a ferric heme protein with molecular weight of 42 kdaltons, experience very fast paramagnetic relaxations with T_1s comparable to those of metMbCN but larger line widths. The heme ^1H NMR resonance assignments of this protein have been based initially upon reconstitution with costly ^2H-labeled hemin,[10] and subsequent assignments are based upon the NOE connectivities from the heme to the protein matrix.[16,17] The ^1H MCOSY spectrum of HRPCN (not shown) exhibits the expected cross peaks between the previously assigned[10,16] heme 7-propionate $C_{\alpha 1}H$:$C_{\alpha 2}H$ and the 4-vinyl $C_\alpha H$:$C_\beta H_2$. The HOHAHA map of HRPCN was less informative (not shown), failing to detect the peaks from 7-propionate which exhibits broader line widths than the vinyl groups.

Discussion

Scope and Limitations. For each of the target residues in the heme cavity of metMbCN, complete identification of the spin system origin could be effected by one or more of the bond correlation 2D methods, except for the His imidazole ring. These bond connectivities involved protons with significant hyperfine shifts (~ -11 to $+15$ ppm) and paramagnetic relaxation ($T_1 \geq 20$ ms and line width ≤ 100 Hz) typical of a low-spin ferric hemoprotein for protons >4 Å from the iron. Excluded from such spin connectivity detection are the F8 His ring protons which exhibit line width ~600 Hz and T_1 ~4 ms and must be identified by 1D NOE methodology.[19] The currently characterized spin connectivities for the residues closest to the iron completely confirm the assignments previously proposed[19] by interpreting the NOESY cross peaks on the basis of crystal coordinates, *except for one prominent exception, Leu F4* (see below). For spins where the relaxation is sufficiently weak to allow detectable two- or three-bond coherence at the end of a suitable mixing period, the HOHAHA map facilitates identification of the whole spin system through the relay at longer mixing times. Paramagnetism imparts an additional advantage for tracing the complete spin connectivity throughout a side chain: the component peaks exhibit substantial and relatively predictable temperature dependence[9,19] so that accidental degeneracies are rather trivially resolved. Hence, complex spin systems can be completely mapped via variable-temperature MCOSY experiments even when HOHAHA is ineffective (see below). It is clear that the assignment of the majority of the paramagnetically influenced residues (except proximal His ring) could have been assigned via the spin connectivity 2D maps conventionally utilized in analyzing comparable diamagnetic proteins, i.e., MbCO.[33]

There is a large class of low-spin ferric hemoproteins, including the genetic variants and, more recently, synthetic point mutants of ferricytochromes, Mbs, and monomeric Hbs, for which it can be expected that complete assignments are now obtainable. For the ferricytochromes, only the main-chain protons for the heme pocket residues have been detected by 2D NMR,[29] and the assignments for the pocket side chains have been generated via saturation transfer via electron exchange from the more readily assignable diamagnetic ferrocytochromes.[12,13] However there exist numerous ferricytochromes for which the electron self-exchange rate is not suitable for such studies,[41-44] hence for which assignments by this method are not attainable. For metMbCN complexes, currently available assignments have been derived from analysis of the NOESY map in terms of crystal coordinates.[19] However, as the present study illustrates, this can lead to erroneous assignments because the solution and crystal structures may differ (see below). Together with the rate of buildup of cross peaks in the NOESY map, the independent assignments by bond connectivity provide, at least hypothetically, the potential for the determination of the three-dimensional solution structures of ferricytochromes, metcyano Mbs, and monomeric Hbs in a manner currently pursued for diamagnetic ferrocytochromes and MbCO.[33,34,45] Our preliminary detection of heme MCOSY peaks for the low-spin ferric HRPCN[10] complex suggests that these methods may be applicable even to the larger heme peroxidases.[16,17] Current efforts are directed toward exploring these possibilities.

Comparative Evaluation of the 2D Methods. The present 2D bond correlation experiments provide all of the data needed to unambiguously identify spin systems of the targeted residues in metMbCN, but the various methods display highly variable information. The data indicate that the optimal strategy for obtaining such assignments may require a variety of such experiments, depending on the information being sought. Table II summarizes the comparative results for detecting the expected spin connectivities for the targeted residues. *Among the common experiments*, MCOSY, DQF-COSY, and HOHAHA, *the highest information content, in terms of the total number of detected cross peaks, is the MCOSY spectrum, where essentially all the expected bond connectivities for the targeted residues are detected.* However, the cross peaks close to the diagonal in the diamagnetic region of the MCOSY map are not resolved because the phase-twisted line shapes[40,46] of the strong diagonal obscure such detection (e.g., heme 7-propionate cross peaks). On the other hand, the connectivities between pairs of the most strongly relaxed resonances, Phe CD1 $C_\zeta H$:$C_\epsilon Hs$ (Figure 2) and Ile FG5 $C_{\gamma 1}H$:$C_{\gamma 2}H$ (Figure 3), are detected. Both of these two cross peaks, however, are missing in the DQF-COSY and HOHAHA maps (Figure 4) regardless of the window functions used. The major difference for cross peaks detectability between the MCOSY and DQF-COSY maps, in fact, depends on the residue of interest. For the weakly relaxed and moderately hyperfine shifted resonances, DQF-COSY is superior to MCOSY because the former can reveal cross peaks very cose to the diagonal. *However, for the rapidly relaxed and strongly hyperfine shifted signals, MCOSY is superior to DQF-COSY (e.g., Phe CD1 $C_\zeta H$:$C_\epsilon Hs$ and Ile FG5 $C_{\gamma 1}H$:$C_{\gamma 2}H$).* The failure to observe those cross peaks in the latter map in the present study is not because of inadequate digital resolution, as commonly suggested in the literature. Instead, we propose that it is due to the effect of the double quantum filter, DQF.

To qualitatively test this hypothesis, we examined the phase-sensitive COSY and PCOSY, which do not include DQF. The phase-sensitive COSY and MCOSY experiments yield essentially identical results except for the antiphase nature of the cross peaks in the former spectrum. The phase-sensitive PCOSY map has improved sensitivity and a narrow diagonal like the DQF-COSY map except for the absence of DQF. In fact, the PCOSY map exhibits all peaks observed on the MCOSY map except that for Phe CD1 $C_\zeta H$:$C_\epsilon Hs$, in addition to allowing detection of cross peaks as close to the diagonal, as in DQF-COSY. However, the difficulty in implementing the PCOSY experiment detracts from its common usage. Figure 5 shows the slices through the rapidly relaxed signal of the Ile FG5/99 $C_{\gamma 1}H$ in metMbCN along the t2 direction from the different bond correlation experiments. It can be seen clearly that the phase-sensitive COSY and PCOSY can detect the Ile FG5 cross peaks $C_{\gamma 1}H$:$C_{\gamma 2}H$ and $C_{\gamma 1}H$:$C_\delta H_3$ even at a digital resolution of 15 Hz/point (Figure 5B,C), while the DQF-COSY simply failed to detect these cross peaks whether the data were processed with the same or higher digital resolution (Figure 5D). *Thus, it can be concluded that the DQF not only removes uncoupled single resonances such as the strong solvent line and methionine SCH_3 but also strongly discriminates against broad J coupled resonances.* Moreover, a coarse digital resolution of 15 Hz/point is shown to be already enough to avoid severe cancellation of the antiphase multiplet structures of those broad signals in the experiments of phase-sensitive COSY and its variants, although a higher digital resolution is required for displaying fine multiplet structures and for precisely measuring coupling constants.

While the phase-sensitive DQF-COSY spectrum has antiphase multiplet structures and MCOSY has twisted line shapes, the HOHAHA spectrum has in-phase multiplet structures and pure absorption line shapes. Thus, the HOHAHA spectrum overall has higher sensitivity and resolution than either COSY spectrum, as expected, *but only for the weakly paramagnetically relaxed lines.* Furthermore, HOHAHA spectra collected with different mixing times can provide unambiguously the *complete identification* of some paramagnetically relaxed amino acid residue spin systems on the bases of coherence transfer within the individual

(41) Moore, G. R.; Williams, J. R. P.; Peterson, J.; Thomson, A. J.; Mathews, F. S. *Biochim. Biophys. Acta* **1985**, *829*, 83–96.
(42) Timkovich, R.; Cork, M. S.; Taylor, P. V. *Biochemistry* **1984**, *23*, 3526–3533.
(43) Timkovich, R.; Cork, M. S. *Biochemistry* **1984**, *23*, 851–860.
(44) McDonald, C. C.; Phillips, W. D.; LeGall, J. *Biochemistry* **1974**, *13*, 1952–1959.
(45) Englander, S. W.; Wand, A. J. *Biochemistry* **1987**, *26*, 5953–5958.
(46) The MCOSY spectrum at a higher contour level has the comparable appearance of the cross peaks as in the DQF-COSY and HOHAHA spectra which are displayed at a lower contour level. However, at a lower contour level for displaying the cross peaks derived from the fast relaxed resonances, the MCOSY spectrum simply hides cross peaks near the diagonal envelop.
(47) Davis, D. G.; Bax, A. *J. Am. Chem. Soc.* **1985**, *107*, 7197–7198.

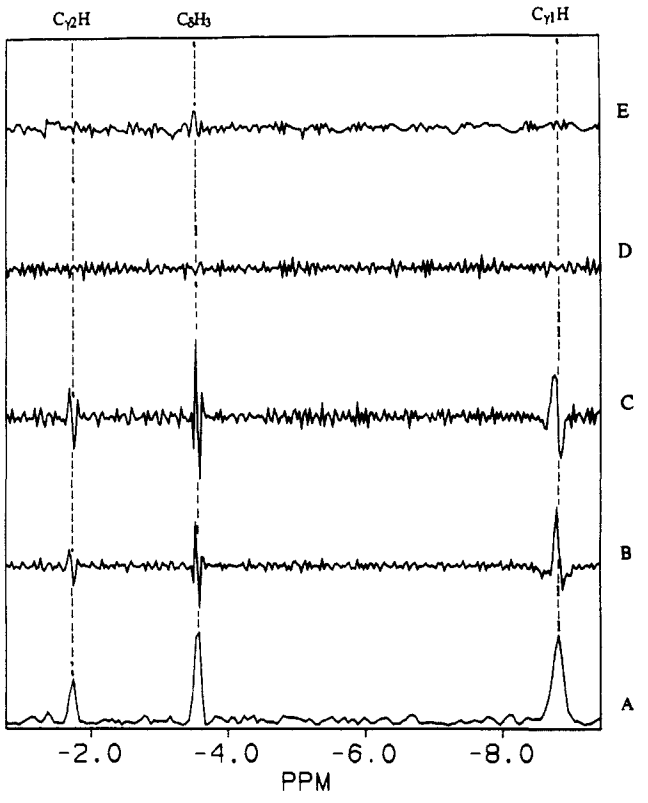

Figure 5. The slices along the t2 direction through the broad resonance of Ile FG5/99 $C_{\gamma 1}H$ of metMbCN at 35 °C from the different bond correlation experiments: (A) MCOSY spectrum, (B) phase-sensitive PCOSY spectrum, (C) phase-sensitive COSY spectrum, (D) phase-sensitive DQF-COSY spectrum, and (E) HOHAHA spectrum collected with 25-ms mixing time and with a trim pulse length of 100 μs. All the 2D spectra shown in this figure are multiplied with a nonshifted sinebell except for the HOHAHA spectrum with a shifted sinebell of 30° and processed up to a digital resolution of 15 Hz per point.

amino acid side chain (i.e., Val E11/68 and Leu F4/89, see Figures 3 and 4) but not others (i.e., Phe CD1 and Ile FG5/99). The disadvantage of HOHAHA relative to COSY variants for detecting cross peaks for strongly relaxed protons is that the *relaxation competes effectively with the development of coherence in the mixing time*, thereby suppressing the development of significant coherence prior to detection, e.g., the two missing cross peaks of Phe CD1/43 $C_{\zeta}H$:$C_{\epsilon}Hs$ (not shown) and Ile FG5/99 $C_{\gamma 1}H$:$C_{\gamma 2}H$ (Figures 3B and 5E). For pairs of J coupled protons where one signal is very broad and the other is relatively narrow, the cross peak between them still can be observed despite the significant signal decay of the broad one, as clearly demonstrated by the presence of the cross peak Ile FG5/99 $C_{\gamma 1}H$:$C_{\delta}H_3$ (Figures 3B and 5E). The signal decay constant in the rotating frame, $T_{1\rho}$, for simple mixing schemes is approximately the laboratory frame T_2.[47] By using the new mixing scheme of MLEV-17,[26] the magnetization decay is reduced slightly but is still predominantly controlled by T_2, not T_1. This point can be clearly illustrated by comparing the relaxation properties of Phe CD1–43 $C_{\zeta}H$ and Ile FG5/99 $C_{\gamma 1}H$: the T_1 values are 20 and 65 ms and the T_2 values are 4 and 3.3 ms (estimated based on the line widths; see Table I). The Ile FG5/99 $C_{\gamma 1}H$ decays faster than the Phe CD1/43 $C_{\zeta}H$ during the spin-lock period (not shown) because of its shorter T_2 relaxation time and despite its longer T_1 relaxation time.

Orientation of Leu F4/89. The earlier assignment[19] of the two Leu F4 signals ($C_{\delta 2}H_3$ and $C_{\gamma}H$) was obtained by interpreting the largest interresidue NOE from His F8 $N_{\delta}H$ to that of Leu F4 $C_{\delta 2}H_3$ on the basis of crystal coordinates, estimated peak intensity, and excellent correlation of the observed extreme low field (~9 ppm) position with predictions based on the dipolar field generated by the determined magnetic axes;[6] the $C_{\gamma}H$ peak was proposed[19] based on the detection of a DQF-COSY peak from the putative $C_{\delta 2}H_3$. The observed shift for this putative Leu F4 $C_{\delta 2}H_3$ was used as input for the determination of the orientation of the susceptibility tensor.[6] The current unambiguous assignment of all of the Leu F4 resonances requires a reassessment. Firstly, deletion of the erroneous Leu F4 $C_{\delta 2}H_3$ data point from the input for the determination of the susceptibility tensor leaves the resulting orientation of the tensor completely unchanged[6] and even slightly improves the quality of fit (i.e., F/n reduces from 0.53 to 0.50). Secondly, the Leu F4 methyl shifts, δ^*_{pre}, predicated by the magnetic axes using the X-ray structure orientation of Leu F4, differ substantially from those, δ_{obs}, measured experimentally by the positions of the cross peaks in the DQF-COSY or HOHAHA maps, as shown in Table III. Moreover, inspection of the variable-temperature NOESY and COSY maps (not shown) reveals that there are NOESY cross peaks between the heme 1-CH_3 and *both* Leu F4 methyls, in spite of the fact the crystal coordinates[20] of MbCO place only $C_{\delta 1}H_3$ sufficiently close to 1-CH_3. Hence we conclude that the solution orientation of Leu F4 is not adequately represented by the solid-state structure.

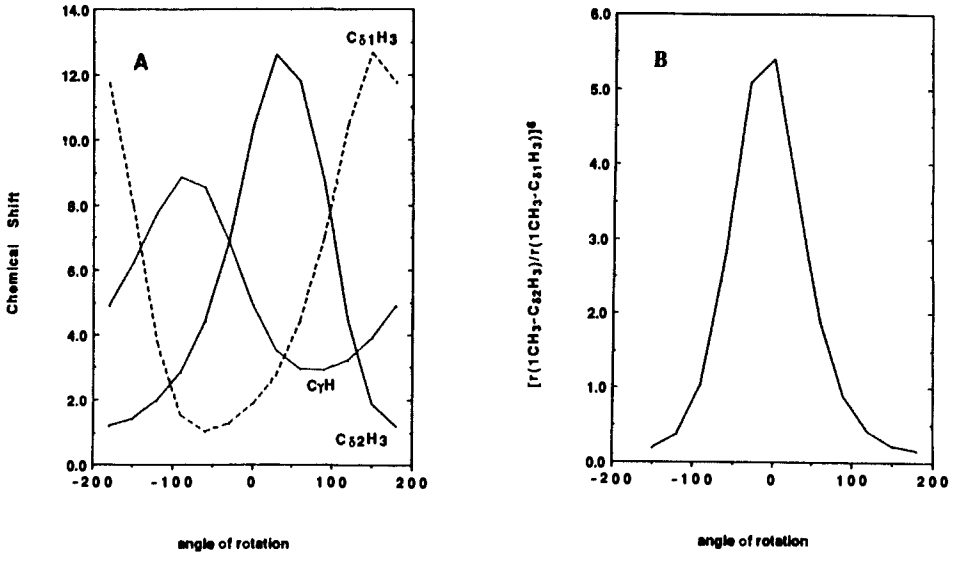

Figure 6. (A) Plot of predicted chemical shifts vs rotation angles of the C_{β}–C_{γ} bond of the Leu F4/89 side chain. The C_{β}–C_{γ} bond is rotated in the positive clockwise direction relative to that in the crystal structure, looking down the C_{β}–C_{γ} bond direction. (B) Plot of the ratio of calculated [r(heme 1-CH_3–Leu F4 $C_{\delta 2}H_3$)/r(heme 1-CH_3–Leu F4 $C_{\delta 1}H_3$)],[6] i.e., the expected NOE ratio from the heme 1-CH_3 to the two Leu F4 methyls as a function of the same bond rotation angle. The observed shifts are best represented for the C_{β}–C_{γ} angle of −120 ± 20° with respect to that in the crystal structure (A), and the angle also predicts comparable NOEs between the heme 1-CH_3 and two Leu F4 methyls (B).

Table III. Chemical Shifts of Leu F4/89 in metMbCN

spins	δ_{obs}[a]	δ^*_{pre}[b]	δ^+_{pre}[c]	δ_{dia}[d]	δ_{dip}[e]	slope ($\times 10^{-3}$)[f]
$C_\alpha H$	8.68	8.46	8.46	3.74	4.94	2.76
$C_{\beta 1} H$	4.51	3.82	3.82	1.48	3.03	1.62
$C_{\beta 2} H$	3.85	3.12	3.12	1.18	2.67	1.14
$C_\gamma H$	6.02	4.86	7.76	0.63	5.39	3.14
$C_{\delta 1} H_3$	4.07	1.86	3.77	0.31	3.76	2.67
$C_{\delta 2} H_3$	3.34	10.36	1.96	0.44	2.90	1.81

[a] Experimentally observed chemical shifts in ppm from DSS at 25 °C in ^2H_2O at pH*8.6. [b] Predicted chemical shifts at 25 °C relative to DSS, $\delta^*_{pre} = \delta_{dia} + \delta_{dip}$(calc), where δ_{dip}(calc) is computed by using the crystal structure orientation of Leu F4; taken from ref 6. [c] Predicted chemical shifts at 25 °C, relative to DSS, $\delta^+_{pre} = \delta_{dia} + \delta_{dip}$(calc), where δ_{dip}(calc) is calculated from the new orientation of the Leu F4 side chain which best reproduces the data (Figure 6). [d] Diamagnetic shifts obtained from MbCO at 36 °C and pH* 5.6 (ref 33). [e] The experimentally observed dipolar shift, $\delta_{dip} = \delta_{obs} - \delta_{dia}$. [f] Slopes were measured from the variable-temperature behavior of the experimentally observed chemical shifts, $\Delta\delta/\Delta(1/T)$ in ppm °C; see ref 6.

Leu F4 lies on the proximal side of the heme adjacent to the "xenon hole", a hydrophobic vacancy over pyrrole I, and hence has available to it significant conformational flexibility, particularly about the C_β–C_γ bond, without disrupting neighboring residues.[20,33] To ascertain whether the failure to predict correctly the Leu F4 dipolar shift is due to a distinct alternate orientation, we calculated both the dipolar shifts and expected NOEs between the Leu terminal methyls and the heme 1-CH_3 (i.e., [r(heme 1-CH_3–Leu F4 $C_{\delta 2}H_3$)/r(heme 1-CH_3–Leu F4 $C_{\delta 1}H_3$)][6]) as a function of the C_β–C_γ rotational angle; the results for these calculations are presented in Figure 6. It is clear from this figure that rotation about the C_β–C_γ by −120 ± 20° not only reproduces reasonably both the pattern and magnitudes of the Leu F4 shifts (δ^+_{pre} at −120° rotational angle; see Table III) but also places both methyls within comparable NOE distance of the heme 1-CH_3, as observed. Moreover, the slopes of the experimental dipolar shifts, derived from variable-temperature COSY maps, are proportional to the dipolar shifts, δ_{dip} (Table III), as found earlier for all other dipolar shifted residues[6] and hence argue not only that the orientation of Leu F4 in metMbCN in solution is different from that of MbCO in the crystal but also that this orientation with C_β–C_γ rotated by ~120° is likely the dominant one. It is of interest that the reoriented Leu F4 presently characterized in solution of sperm whale metMbCN is close to that found in the crystal structure of horse metMb:[48] the horse and sperm whale Mb crystal structures are otherwise isostructural on the proximal side of the heme pocket. Hence this residue provides a dramatic example of the problem that can arise when solution NOESY data are interpreted too closely on the basis of crystal coordinates and reaffirms the absolute necessity for the independent amino acid spin connectivity assignments provided by the present study.

Acknowledgment. The authors are indebted to S. D. Emerson who wrote the computer programs for dipolar shift calculations. This research is fully supported by a grant from the National Institutes of Health, HL-16087.

(48) Evans, S. V.; Brayer, G. D. *J. Biol. Chem.* **1988**, *263*, 4263-4268.

Spectroscopic and Chemical Studies of the Laccase Trinuclear Copper Active Site: Geometric and Electronic Structure

James L. Cole, Patrick A. Clark, and Edward I. Solomon*

Contribution from the Department of Chemistry, Stanford University, Stanford, California 94305.
Received June 28, 1990

Abstract: Laccase contains four Cu atoms: a type 1, a type 2, and a coupled binuclear type 3 center. The type 2 and type 3 centers comprise a trinuclear Cu cluster which is thought to represent the active site for the binding and multielectron reduction of dioxygen. A combination of electronic spectroscopy, magnetic susceptibility, and exogenous ligand perturbation has been used to probe the geometric and electronic structure of the trinuclear site. A type 1 Hg^{2+}-substituted laccase derivative was employed in order to remove the overlapping spectral contributions from the type 1 Cu^{2+}. The ligand-field and charge-transfer transitions of the type 2 and type 3 coppers were assigned by use of absorption, circular dichroism, and low-temperature magnetic circular dichroism spectroscopies. The ligand-field transition energies indicate that all three coppers have tetragonal geometries and that the two type 3 coppers are inequivalent. Magnetic susceptibility measurements have defined the lower limit for the magnitude of the exchange interaction between the type 3 coppers and have probed type 2–type 3 interactions. Binding of the exogenous ligand azide to the trinuclear site produces characteristic azide → Cu^{2+} charge-transfer features and also perturbs the type 2 and type 3 ligand-field transitions. Analysis of these spectral features demonstrates that azide binds as a bridging ligand between the type 2 site and one of the type 3 coppers. In addition, a second azide coordinates to the type 3 site with a lower binding constant, and this second azide also strongly interacts with the type 2 site. The type 2–type 3 bridged binding of azide suggests that a similar coordination mode is active in the irreversible binding and four-electron reduction of dioxygen. The second azide binding provides a further demonstration of the differences between the laccase type 3 site and the coupled binuclear sites in hemocyanin and tyrosinase. A model for the magnetic interactions among the three coppers in the resting and ligand bound forms of the trinuclear site is presented.

Introduction

The multicopper oxidases[1,2] laccase, ascorbate oxidase, and ceruloplasmin catalyze the four-electron reduction of dioxygen to water. The Cu atoms present in these enzymes have been classified[1] according to their EPR features: type 1 or blue ($A_\parallel \leq 95 \times 10^{-4}$ cm^{-1}), type 2 or normal ($A_\parallel > 140 \times 10^{-4}$ cm^{-1}), and type 3 or coupled binuclear (EPR undetectable). The type 3 coppers are strongly antiferromagnetically coupled so that the type 3 site is diamagnetic, even at room temperature.[3] The superexchange interaction is mediated by an endogenous bridging ligand OR^-.[2] The various copper sites also give rise to characteristic

(1) (a) Malkin, R.; Malmström, B. G. *Adv. Enzymol.* **1970**, *33*, 177. (b) Malmström, B. G.; Andréasson, L.-E.; Reinhammar, B. In *The Enzymes*; Boyer, P. D., Ed.; Academic: New York, 1975; Vol. XII. (c) Fee, J. A. *Struct. Bonding (Berlin)* **1975**, *23*, 1-60.

(2) Solomon, E. I.; Penfield, K. W.; Wilcox, D. E. *Struct. Bonding (Berlin)* **1983**, *53*, 1.

(3) Dooley, D. M.; Scott, R. A.; Ellinghaus, J.; Solomon, E. I.; Gray, H. B. *Proc. Natl. Acad. Sci. U.S.A.* **1978**, *75*, 3019-3022.

0002-7863/90/1512-9534$02.50/0